NOTCH-pathway inactivation reprograms oral-stem-like cancer cells to JAK-STAT dependent state and provides the opportunity of synthetic lethality

Subhashis Ghosh
National Institute of Biomedical Genomics
Paromita Mitra
National Institute of Biomedical Genomics
Uday Saha
National Institute of Biomedical Genomics
Arnab Ghosh
National Institute of Biomedical Genomics
Nidhan Kumar Biswas
National Institute of Biomedical Genomics
Shantanu Saha Roy
National Institute of Biomedical Genomics
Moulinath Acharya
National Institute of Biomedical Genomics
Sandeep Singh (ss5@nibmg.ac.in)
National Institute of Biomedical Genomics PO: NSS

Research Article

Keywords: Oral cancer, Stemness, Cellular plasticity, NOTCH-HES, JAK-STAT, Synthetic lethal pair, Targeted therapy

Posted Date: September 14th, 2022

DOI: https://doi.org/10.21203/rs.3.rs-2049980/v1

Abstract

Background: Stem cell-like properties in cancer cells are found to be responsible for its aggressive behaviour. However, this has not been studied with respect to the bimodal NOTCH-pathway-activity status, found in oral cancer.

Methods: Oral-SLCCs were enriched in 3D-spheroids. Constitutively-active and inactive status of NOTCH-pathway was achieved by genetic or pharmacological approaches. RNA sequencing and real-time PCR was performed for gene expression studies. *in vitro* cytotoxicity assessments were performed by AlamarBlue assay and *in vivo*effects were studied by xenograft growth in zebrafish embryo. The *t* tests were performed to estimate statistical significance of the study.

Results: Here, we have demonstrated the stochastic plasticity on NOTCH-activity axis; maintaining both NOTCH-active and inactive states of oral stem-like cancer cells (Oral-SLCCs). While Oral-SLCCs with inactive NOTCH-pathway status showed higher proliferation and aggressive tumor growth, the Cisplatin refraction was associated with active-status of NOTCH-pathway; suggesting the crucial role of plasticity on NOTCH-axis. The differentially expressed genes between NOTCH-pathway active and inactive clones clearly suggested the upregulation of JAK-STAT signaling in subset of Oral-SLCCs with lower NOTCH-pathway activity status. Confirming the function; the 3D-spheroids generated by oral-SLCCs with lower NOTCH-activity-status displayed significantly higher sensitivity to JAK-selective drugs, Ruxolitinib or Tofacitinib and siRNA mediated downregulation of tested partners STAT 3 and 4. Therefore, we adopted the strategy of synthetic lethality, where Oral-SLCCs were reprogrammed to maintain the inactive status of NOTCH-pathway by exposure to γ-secretase inhibitors, LY411575 or RO4929097 followed by targeting with JAK-inhibitors, Ruxolitinib or Tofacitinib. This resulted in a very significant inhibition in viability of 3D-spheroids as well as xenograft formation in Zebrafish embryos; whereas inhibition of either of these pathway alone were largely ineffective.

Conclusion: We have demonstrated the stochastic cellular plasticity on NOTCH-activity axis. Study revealed for the first time that NOTCH-HES and JAK-STAT pathways may act as synthetic lethal pair, and as novel targets against diverse states of stemness in oral cancer. Therefore, we have provided the rational for sequential combination of NOTCH and JAK inhibitors as possible therapeutic strategy against aggressive oral cancer.

Background

A subtype of head and neck squamous cell carcinoma (HNSCC), originating in the buccoalveolar sulcus or gingivolabial sulcus of oral cavity has high prevalence in Pacific Islands and in whole South Asian countries and emerging in other parts of the world, as well (1–4). While it is the eighth most common cancer worldwide; it is the most prevalent cancer among men and fourth most common among women in India (5, 6). Although there is improvement in treatment strategies; mainly surgery and chemo-radiation therapy; majority of the oral cancer patients develop loco-regional secondary and/or metastatic disease,

with very poor post-recurrence survival (5, 7, 8). Cancer cells with stem cell-like properties of long-term self-renewal and differentiation, collectively known as ‘stemness’; are shown to be responsible for cancer initiation, progression, metastasis, resistance to treatment and recurrence after therapy. Therefore, stem cell biology of cancer provides conceptual framework to understand the aggressive behaviour of cancer (9–14). The present study focused to explore the status of NOTCH-pathway activation and its relation with ‘stemness’ in oral cancer cells.

Mutation in *NOTCH1* gene has been implicated in leukaemia, breast cancer and various squamous cell carcinomas including, esophagus, cervix, skin and lung other than HNSCC (15–19). Importantly, the NOTCH-mutation patterns are contrastingly different between these cancer types. In T-cell acute lymphoblastic leukaemia (T-ALL) majority of the truncating mutations occur in the C-terminal domain of the Notch receptor protein, whereas the truncating mutations are commonly located in the ligand binding extracellular domain of the NOTCH receptors in HNSCC including gingivobuccal oral cancer. The NOTCH mutation in HNSCC hampers the ligand-receptor interaction and leads to inactivation of NOTCH1 signaling, contrasting to activation of NOTCH1 in T-ALL (20, 21). Supporting the tumor suppressive role of NOTCH1, conditional loss of function phenotype of NOTCH1 has been shown to result in cutaneous squamous cell carcinoma in mice (22, 23). Although activating mutation in NOTCH-pathway genes is largely lacking in HNSCC; studies have shown that NOTCH1 is significantly upregulated in neoplastic cells compared to normal tissue (24–27). The putative oncogenic role of NOTCH-signaling has been experimentally proven, where blocking of NOTCH1 has led to decrease in cell proliferation, 3D-spheroid growth and xenograft formation in HNSCC cell lines with wild-type status of *NOTCH1* (28, 29). Collectively, these observations are suggesting the bimodal action of active NOTCH-pathway; acting as tumor promoter or suppressor, depending on the cellular context in oral cancer.

Studies have shown a positive correlation between higher-expression of NOTCH-pathway genes and cancer stem cell markers aldehyde dehydrogenase (ALDH) and SOX2 in HNSCC cell lines, supporting the oncogenic role of NOTCH-pathway (30, 31). However, loss of function of NOTCH1 had resulted in outgrowth of basal-stem cells in mouse; suggesting the tumor suppressor role of NOTCH pathway. Immunohistochemistry studies have also found heterogeneous expression of NOTCH1 (ICN1) and its downstream member of HES1 and HEY1; giving evidences of activation of NOTCH-pathway in subsets of cells in several HNSCC tumor sections (29, 32). Thus, while stemness in oral cancer may be dependent on the active NOTCH-signaling in a subset of cancer cells, it may be in maintained in NOTCH-independent manner with loss of function status in other subsets. Therefore, exploring the maintenance of stemness in this diverse background may provide novel target against stemness in oral cancer (33–37).

Here, we have provided the evidence of co-existence of oral-stem-like cancer cells (Oral-SLCCs) with both NOTCH-active and -inactive states. While the sustained activation of NOTCH1 and Hes1 was found to be responsible for Cisplatin-tolerance in Oral-SLCCs; NOTCH-inactivation displayed a transcriptionally distinct state of stemness with aggressive, tumor-promoting functions with activation of JAK-STAT signaling. Harnessing this plasticity, we pharmacologically drove Oral-SLCCs to accumulate in NOTCH-inactive state; rendering them to be dependent on JAK-STAT pathway. Overall, we have provided a novel

strategy of reprogramming Oral-SLCCs to be sensitive to JAK-inhibitors by modulating the NOTCH-activation.

Results

Stemness is maintained by oral cancer cells with both NOTCH-pathway active and inactive status: In our recent report, oral cancer cells with the widely reported phenotype of putative oral SLCCs ($CD44^{+ve}/CD24^{Low}$ or ALDH-High), as well as other possible subpopulations of the cells with $CD44^{+ve}/CD24^{High}$ as well as ALDH-Low phenotypes were able to form the 3D-spheroids and maintenance of hybrid states of Oral-SLCCs (38). Therefore for this study, we adopted the phenotype-free enrichment of Oral-SLCCs in 3D-spheroid cultures from different oral cancer cell lines and checked the expression level of stemness related genes. The adherent cultures were used as control. Quantitative real time polymerase chain reaction (qRT-PCR) results showed significant upregulation for NOTCH-pathway receptor *NOTCH1* and major downstream genes *HES1* and *HEY1* (Supplementary Figure S.1) along with other stemness genes *ALDH1A1, SOX2, cMYC and KLF4* (Supplementary Figure S.1). These observations demonstrated the enrichment of Oral-SLCCs with NOTCH-pathway activation in the 3D-spheroid cultures of oral cancer cells and confirmed the suitability of the cellular models for this studies. We, next explored the effect of Notch-inactivation over the sphere forming ability of oral-cancer cells. Cells were seeded along with the γ-secretase inhibitors LY411575 (LY) or RO4929097 (RO) at given concentration. Interestingly, the sphere forming efficiency was significantly enhanced in the Notch-inhibited conditions compared to the control, for all three tested cell lines SCC029, SCC032 and SCC070 (Figure: 1A-C). siRNA mediated transient knockdown of *NOTCH1* and *HES1* in SCC070 also showed the similar results os higher sphere forming efficiency compared to control siRNA (Supplementary Figure S.2). qRT-PCR analysis of the spheroids, generated with 5μM LY or RO in tested cell lines GBC02 and SCC070, demonstrated downregulation of *NOTCH1* and *HES1* expression, suggesting the inhibition of NOTCH-activity in these cells. Importantly, these NOTCH-inhibited spheroids showed downregulation in stemness factors *SOX2*, *ALDH1A1* and basal cell cytokeratin marker *CK14*, while upregulation of stemness factors *SOX9* and differentiation marker *CK10* (Figure 1D-E). Therefore, results indicated the possibility of the maintenance of an alternative state of stemness in oral cancer cells after Notch-inactivation.

To stably maintain the NOTCH-active status in oral cancer cells we used lentiviral vectors to express the active-intracellular domain of human-NOTCH1 (hICN) or human-Hes1 (hHes1); while for constitutively inactivated status of NOTCH-pathway, a dominant negative form of human-Hes1 (BHes1) was expressed in GBC02 and SCC070 cell lines. As anticipated, the sphere formation efficiency of BHes1 clones was significantly higher compared to both hICN and hHes1 clones for both GBC02 and SCC070 (Figure 1F-G). qRT-PCR analysis further confirmed the observations obtained from spheroids generated with LY or RO (Figure 1 D, E). Both SCC070 and GBC02 cell lines exhibited significant upregulation in *NOTCH1*, *HES1*, *ALDH1*, *SOX2* and *CK14* for hICN and hHes1 clones; whereas, significant increase in *SOX9* and *CK10* and *Involucrin* was demonstrated by NOTCH-inactivated BHes1-clones for both the cell lines (Figure 1 H). Importantly, *in vivo* xenotransplantation of cancer cells with constitutive activation of

NOTCH-pathway (hICN and hHES1) or with inactivation (BHes1) clearly suggested the tumorigenic ability of SCC070 cells, irrespective of NOTCH-pathway status (Figure 1I). NOTCH-pathway inactivated cells resulted in more aggressive tumor, indicated by a significantly poorer survival in zebrafish embryo, post transplantation (Figure 1J). In concordance with this observation, poor prognosis for HNSCC patients having lower expression of *NOTCH1* was found in survival analysis as compared to the patients with its higher expression in The Cancer Genome Atlas (TCGA) study-cohort (Figure 1K).

Spontaneous co-existence of Notch-pathway active and -inactive cell population in OSCC:

Morphologically, spheroids generated from SCC070 cell lines were less diffused than the spheroids generated from other oral cancer cell lines. Therefore, we clearly observed that the spheroids generated from NOTCH-pathway inactive SCC070-bHES1 clones were having higher frequency of larger spheroids than the NOTCH-pathway-active SCC070-hHES1 clone. As shown in Figure 2A, the bHES1 clone had significantly higher number of larger

spheroids with diameter of 100μ or more in all the three different generations, tested here. Since, spontaneously generated spheroids always demonstrate variations with respect to their diameter, this observation intrigued us to explore further. From the spontaneously generated SCC070 spheroids; we collected smaller spheroids of 40-70μm in diameter and larger spheroids with 100μm or more in diameter to perform gene expression analysis. Surprisingly, these two subpopulations showed differential expression in stemness and differentiation related genes (Figure 2B). More interestingly, the *HES1* expression was downregulated in larger spheroids (Figure 2B). The expression of other tested genes, *ALDH1A1, SOX2, cMYC, CK10* and *CK14* showed gene expression pattern, like the NOTCH-pathway-inactive clone (Figure 2B). We next tested if these two sub-types of spheroids can regenerate to its original size after dissociation and replanting. To our surprise, cells dissociated from $1^{'}$ (primary) spheroids with <70μm diameter could also generate the larger spheroids of >100μm, as well as vice versa (Figure 2C). These results suggested the possibility of co-existence and spontaneous interconversion of NOTCH-pathway active (enriched in smaller spheroids) and NOTCH-pathway inactive (enriched in larger spheroids) oral cancer cells, under 3D cell culture condition.

Transitioning to NOTCH-pathway active state provides cisplatin tolerance in Oral-SLCCs:

Previous reports have shown that activation of NOTCH-pathway confers resistance against cisplatin in HNSCC (39,40). Thus, we next tested if oral cancer cells harness its ability to transition between NOTCH-pathway -inactive and -active states to achieve the drug tolerance. As shown in schematic (Figure 2E), OSCC cells, SCC029, SCC032 and SCC070 were plated for spheroid formation. Cisplatin was added at a physiologic dose of 2μM, after the spheroids reached the average diameter of 60μm in 5-7 days after single cell plating. All the tested cell lines showed refraction to cisplatin treatment, as non-significant change in cell viability was observed (Supplementary Figure S.3). Spheroids exposed to cisplatin for 48 hrs were collected for RNA isolation. Parallelly, cisplatin treated spheroids were collected, dissociated into single cells and re-seeded to generate $2^{'}$ (secondary) spheroid, without cisplatin. After 7 days, plated cells

generated 2′ spheroids which were collected for RNA isolation. As anticipated, Cisplatin treatment resulted in significant upregulation of *NOTCH1* and *HES1* expression along with other stemness marker *ALDH1A1, SOX2, SOX9* and differentiation marker *CK1* (Figure 2F). Surprisingly, the increased levels of these tested genes remained upregulated in 2′ spheroids generated from cisplatin treated 1′ spheroids; even when 2′ spheroids were generated without cisplatin (Figure 2F).

These results suggested that the tolerance against cisplatin may be a result of a more stable NOTCH-pathway active status after cisplatin treatment. Therefore, blocking of NOTCH-pathway before cisplatin treatment may result in better efficacy. To test this possibility, we added the γ-secretase inhibitors LY and RO at the time of seeding for spheroid formation of SCC029, SCC032 and SCC070 to block these cells from undergoing cisplatin-induced transition towards a NOTCH-pathway active status. After 5 days of spheroid formation, 2 μM cisplatin was added. Interestingly, compared to the spheres generated in DMSO where cisplatin tolerance was observed; significantly lower spheroid number and reduced viability was achieved for the spheroids, which were generated with inhibited NOTCH-pathway (Supplementary Figure S.3). Encouraged from these results, we performed the cisplatin sensitivity assay to quantitate the difference in cisplatin efficacy by calculating IC_{50} value of Cisplatin in combination of 5 μM of γ -secretase inhibitors for both GBC02 and SCC070 cell lines (S.4). Similarly, IC_{50} value was calculated by making comparison between constitutively NOTCH-pathway active (hICN) and -inactive (BHES1) clones of GBC02 and SCC070 cell lines (Supplementary Figure S.4). Both these experiments demonstrated the significant reduction in IC_{50} value for cisplatin in NOTCH-pathway inactive cells as compared to NOTCH-pathway active cells in both the cell lines (S.4). Thus, our results strongly suggested that oral cancer cells adapt to the cisplatin treatment by transitioning to the drug tolerant state through activation of NOTCH-pathway, as one of the possible mechanisms.

NOTCH-pathway inactive state of Oral-SLCCs showed increased JAK-STAT signaling:

We next explored the differential expression of genes between spheroids of NOTCH-pathway active and inactive status of Oral-SLCCs to understanding the responsible mechanism of maintenance of stemness and spontaneous transitioning between these subpopulations. Spheroids were generated form constitutively NOTCH-pathway active (hICN) and -inactive (BHES1) clones of SCC070 cell line and RNA was subjected for RNA sequencing (RNAseq). Among the differentially expressed genes (DEGs), 238 genes were significantly upregulated in NOTCH-pathway active spheroids whereas, 800 genes were significantly upregulated in NOTCH-pathway inactive spheroids with log2 fold change of more than 1 with p value of less than 0.05 (Supplementary Table 1). Interestingly, the NOTCH- pathway inactive spheroids revealed a significant enrichment of inflammatory responsive genes in gene set enrichment analysis (Supplementary Table 2; Figure 3A). DEGs in NOTCH-pathway inactive spheroids showed enrichment of gene sets of interferon alpha signalling and inflammatory response (Figure 3B i-ii). Supporting the activation of JAK-STAT pathway, KEGG JAK-STAT signaling dataset from GSEA-MSigDB showed significantly higher overlap with DEGs in NOTCH-pathway inactive spheroids as compared to NOTCH-pathway active spheroids (Figure 3C). Recently we have demonstrated the emergence of hybrid

state of stemness in oral cancer cells with co-expression of stemness and differentiation associated genes (38). Since, inhibition of NOTCH-pathway showed the similar pattern of expression, we next explored the overall similarities by overlapping the upregulated genes in NOTCH-pathway inactive cells with the upregulated gene sets of putative Oral-stem-like cancer cells (Oral-SLCCs) and hybrid state of stemness in oral-SLCCs (38). Interestingly, the upregulated genes in NOTCH-pathway inactive cells showed significantly higher overlap with hybrid state of Oral-SLCCs (Figure 3D).

To confirm the induction of JAK-STAT signalling in NOTCH-pathway inhibited spheroids, immunoblotting was carried out for key downstream STAT proteins. Spheroids were treated with 5 μM concentration of LY or RO for 48 hrs before harvesting and total as well as phosphorylated forms of STAT1, STAT3 and STAT4 was tested. All three tested STATs were found to be phosphorylated in NOTCH-pathway inactivated cells as compared to DMSO control (Figure 3E). These results imply that the JAK-STAT signalling is activated in NOTCH-pathway inhibited condition in Oral-SLCCs. Collectively, our results suggested for the first time that the inactivation of NOTCH-pathway in oral cancer cells may reprogram the oral-SLCCs to acquire a hybrid-state of stemness with activation of JAK-STAT signalling.

Inhibition of JAK-STAT signal suppresses stemness in NOTCH-pathway inactive state of Oral-SLCCs: Activation of JAK-STAT signaling in NOTCH-inactive condition may be responsible for maintenance of stemness in these hybrid and more aggressive state of oral-SLCCs, as explained earlier. To explore this hypothesis, we first performed siRNA mediated knockdown of two of the major downstream effectors STAT3 and STAT4 in NOTCH-pathway active (hICN) and inactive (BHes1) clones of SCC070 and GBC02 cell lines. After 48 hrs of incubation with siRNA these cells were harvested and plated for sphere formation. Although with similar levels of knockdown in both the clones for both genes (Supplementary Figure S.5); interestingly, while knockdown of STAT3 or STAT4 did not result in loss of sphere forming efficiency in hICN clones; significant loss in sphere formation efficiency was observed in BHes1 clones for both the cell lines (Figure 4A i-ii). For quantitative representation we used viability of the spheres estimated by AlamarBlue assay as a measure. As anticipated, hICN clones did not show any difference in viability; whereas, BHes1 clones had significantly less viability after STAT3 or STAT4 siRNA transfection for both the cell lines, (Figure 4B i-ii).

The JAK-STAT pathway silencing showed more efficient inhibition of stemness in Oral-SLCCs with NOTCH-pathway inhibited status; clearly suggested the synthetic lethal interaction between these two pathways. This prompted us to investigate the sphere forming efficiency of oral cancer cell with potent and selective JAK inhibitors, Ruxolitinib (Ruxo) or Tofacitinib (Tofa) to pharmacologically block JAK-STAT signalling. The hICN and BHes1 clones from GBC02 and SCC070 were plated for sphere formation in presence of the JAK inhibitors. DMSO was used as control. The sphere formation was followed for 7 days and representative images of spheroids generated in each condition is given as supplementary figure S.6. Similar to the observations obtained from siRNA mediated knockdown, JAK inhibitors did not have any significant effect on sphere size or viability in hICN clones for both the cell lines (Figure C i-iv). Under similar conditions, both the JAK inhibitors significantly suppressed the sphere forming ability of

BHes1 clones for both the cell lines. Overall, these results clearly suggested the involvement of JAK-STAT signaling in maintenance of stemness in Notch-pathway inactive population of oral-SLCCs.

Inhibitory effect of JAK-STAT signaling inhibition on the cells with inactive NOTCH-pathway strongly demonstrated that these two pathways may act as synthetic lethal pair against oral-SLCCs. Therefore, to explore this possibility we tested three different cell lines GBC02, SCC029 and SCC070 using the pharmacological inhibitors to block NOTCH- and JAK-STAT pathways. First, these small molecule were added at single cell stage and spheroid formation was monitored for 5 days without renewing the drugs. Representative images of generated spheroids under each condition is given in supplementary figure S.7. The generated spheroids were quantified by AlamarBlue and given in Figure 5A. As expected, inhibition of NOTCH-pathway by LY or RO did not result in loss of sphere formation and viability; whereas, both the JAK inhibitors (Ruxo or Tofa) significantly suppressed sphere formation in GBC02 and SCC029 cells. Interestingly, all the three tested cell lines demonstrated significant higher abrogation of sphere forming efficiency when a combination of LY or RO was used with Ruxo or Tofa (Figure 5A i-iii).

Encouraged from these results, we next tested the efficacy of synthetic lethal approach on the spheroids after growing to the size on 60 µm or more, for three different cell lines. First, the spheroids were allowed to grow for 5 days for it to reach to the size of 60 µm or more. LY, RO, Tofa or Ruxo was added to the respective well alone or in combinations as indicated (Figure 5B, S.8) for 48 hrs. Very interestingly, the NOTCH or JAK pathways inhibition alone did not result in any significant loss in the spheroids viability; however, the combination of both the pathways showed significant loss in spheroid size and viability (Figure 5B i-iii, Supplementary Figure S.8).

Loss in spheroids growth clearly suggested the inhibition of stemness in oral cancer cells by co-inhibition of NOTCH and JAK-STAT signaling. Thus, we tested the effect of this synthetic lethal pair on inhibition of tumor-initiating ability of oral cancer cells in the zebrafish embryos. We treated the hICN and BHes1 clones of SCC070 cell line with the JAK inhibitors or DMSO under adherent culture conditions for 48 hrs. Cells were harvested and inoculated into zebrafish embryos (48 hours post fertilization (hpf)). For each condition, we took 14-15 embryos. Embryos were monitored for 5 days and images of the tumor bulk were taken under fluorescence microscopy on day 3 and 5, post-inoculation. As observed previously, the BHes1 clones generated more aggressive cancer as compared to the hICN clones (Figure 5C). Further, the BHes1 harbouring embryos showed poorer survival (Figure 5D). Interestingly, the Ruxolitinib and Tofacitinib treated cells had resulted in localized tumor formation and significantly reduced tumor bulk as compared to DMSO treated cells (Figure 5C). Also, the JAK inhibitor treated hICN and BHes1 clones had higher number of live zebrafish embryos post inoculation (Figure 5D), it was significantly ($p= 0.04$ & $p= 0.02$) higher for bHES1 clones. These results indicated that the JAK inhibitors may potentially be used to control the aggressive properties of oral tumors in combination with NOTCH-pathway inhibition.

Discussion

Cancer stem cell model suggests that the tumors cells are hierarchically organized, where SLCCs display tumorigenic potential and occupy the top of the hierarchy. Through asymmetric cell division, SLCCs self-renew themselves and differentiate into progenitor-like cells with higher proliferating property. The bulk of the tumor population is differentiated cells and placed in bottom positions having with non-tumorigenic ability (41, 42). However, subsequent recent studies have provided evidences of cellular plasticity; where property of stemness may be achieved over time by differentiating subpopulation of cancer cells; therefore, has challenged the unidirectional hierarchical model of cancer stem cells (43–46). Recently, we have demonstrated similarities between hierarchal structure of normal mice oral mucosal basal layer and population trajectories of oral cancer cells (38). In addition to harbouring oral epithelial progenitor cells (OEPCs), the basal layer also accommodates maturing keratinocytes with co-expression of high levels of cytokeratin 14 (CK14) and genes associated with both OEPCs and differentiation processes, representing transitional intermediated cell states in basal cells of oral epithelium (47). Similarly, transcriptome states of different phenotypic subpopulations derived by combining CD44, CD24 and Aldehyde dehydrogenase activity (ALDH) phenotypes demonstrated that Oral-SLCCs were not limited to specific phenotypic compartment but co-existed as transitional hybrid cell states with alternate phenotypes of differentiating oral cancer cells. In our present study, we have provided the evidence of spontaneous transitioning of oral-SLCCs on NOTCH-pathway activity axis (Fig. 2). Importantly, the inhibition of NOTCH-pathway activity showed shifting of Oral-SLCCs towards hybrid state of stemness (Fig. 3). This observation suggested that spontaneous inhibition of NOTCH-pathway may act as one of the mechanisms to acquire alternate states of stemness in oral cancer cells. Maintenance of both active as well as inactive status of NOTCH-pathway in oral cancer spheroids could be due to the lateral inhibition of NOTCH-signaling induced by differential expression of NOTCH-receptor and -ligands and negative feedback between these signaling molecules in oral cancer cells, as demonstrated in glioblastoma cells (48). However, this possibility needs to be tested in future studies.

Crucially, the cellular plasticity is emerging as survival strategies, adapted by cancer cells, allowing to transit to drug tolerant stem cell-like states in response to the stress induced by chemotherapeutic drugs, in multiple cancers including oral cancer. Few of the earlier studies have demonstrated the activation of NOTCH-pathway to be responsible for resistance against Cisplatin in oral cancer cells. In our study, transient exposure to a sublethal dose (2μM) of Cisplatin was sufficient to induce higher expression of *NOTCH1/HES1* in 3D-spheroids which remained elevated even in the next generation of spheroids formation without exposed to Cisplatin. Therefore, we have emphasized that the Cisplatin-refractory oral-SLCCs switch to activated status of NOTCH-pathway to acquire drug tolerant state. Supporting to this notion, Cisplatin selected oral cancer cells were found to express higher levels of SOX9 in an earlier study; which is similar to our result, where SOX9 expression was elevated in spheroids after treatment with sublethal dose of Cisplatin (Fig. 2). The SOX9 expression remained higher in the 2nd generation of spheroids, generated from these Cisplatin refracted cells even in absence of Cisplatin. Thus, plasticity on NOTCH-activity axis may provide the ability to Oral-SLCCs to emerge as drug tolerant population. Thus, targeting this switch along with chemotherapy may provide better treatment outcome for oral cancer patients.

For better understanding of the molecular difference between Oral-SLCCs with Notch-pathway active or -inactive status, we performed RNA sequencing experiment. Activation of JAK-STAT pathway was found to be significantly upregulated with NOTCH-Low status (Fig. 3). The activation of JAK-STAT signaling in oral-SLCCs may have strong clinical significance. While some studies have shown the suppressive role (49, 50); several studies have provided evidence of activation of JAK-STAT signaling in oral cancer progression, cancer cell proliferation, invasion and immunosuppression (51–54). Role of JAK-STAT signaling as a crosslinker with other stemness regulating signaling pathways to confer self-renewal, epithelial to mesenchymal transition and drug-resistance has been reported in various other cancer (55–60). In the present study, Oral-SLCCs with NOTCH-inactivated status displayed higher proliferation and sphere forming efficiency as well as generation of more invasive xenografts in the zebrafish embryo, with poor survival of tumor bearing embryos (Fig. 1), supporting the tumor promoting role of activated JAK-STAT signaling in oral cancer. Downregulation of STATs or pharmacological inhibition of JAKs in NOTCH-inactivated oral-SLCCs significantly abrogated the sphere-forming ability and aggressive behaviour of xenografts in zebrafish; clearly suggested that active JAK-STAT signaling is responsible for maintenance of stemness in NOTCH-inactivated condition.

Interplay between NOTCH-pathway and JAK-STAT signaling has been shown to play pivotal role in cell fate determination during development process. Genetic interaction between these two signalling pathway seems to be highly diverse. Depending on the developmental context, these two pathways interact either as upstream or downstream regulators of each other (61). Like, active JAK-STAT signaling was shown to be responsible for proliferation of intestinal stem cells (ISCs) in *Drosophila*. The activated NOTCH-pathway is found to restrain the JAK-STAT signaling through downregulation of its signaling activator *unpaired* (*upd*), resulting in differentiation and suppression of proliferation in ISCs (62). However, active JAK-STAT signaling is shown to activate NOTCH-pathway and proliferation of ISCs in response to bacterial infection in the gut (63). On the other hand, in *Drosophila* ovary, the JAK-STAT dependent stalk-cells and NOTCH-dependent main-body follicle cells setup the boundary between them by mutual inhibition of these pathways (64). In vertebrates, a synergy between these two pathways was demonstrated in neuroepithelial cells of mouse. Here, the Hes1 protein is found to act has cytoplasmic scaffold protein to physically interact with STAT3 and recruit it to JAK2 for phosphorylation of STAT3 in neuroepithelial cells (65). Interplay between these two signaling pathways is also found in Toll-like receptors (TLRs) mediated activation of human primary monocytes. In response to the bacterial infection of after TLR induction, NOTCH-ligand, DLL1 expression was found to be driven by STAT3 mediated transcription. In positive feedback manner, recombinant DLL1 was responsible for STAT3 phosphorylation in monocytes. Collectively, these results clearly suggested the NOTCH and JAK-STAT pathways interact in context dependent manner for driving important and diverse physiological effects. Thus, interplay between these two important signaling pathways may play important role in cancer; however studies are largely missing. A report in breast cancer cells has demonstrated the non-canonical activation of NOTCH as upstream regulator of IL6 mediated activation of JAK-STAT pathway (66). Our observation are suggesting the possibility of lateral inhibition and bidirectional cross-talk between signal-sending and receiving cells, resulting in spontaneous existence of NOTCH-active and inactive

subpopulations with differential status of JAK-STAT signaling and overall state-transition in oral-SLCCs. Therefore, it will be crucial to investigate the intermediate molecular events connecting these two pathways in cancer cells as well as spatial arrangement of these diverse subpopulation within the tumor.

Further, an elegant study by Longanathan et al. clearly demonstrated that the NOTCH-pathway inactivation is a common event in HNSCC, even when the components of the pathway are not directly mutated or involved (67). This study has estimated that 67% of human HNSCC patients have inactive status of NOTCH-pathway. Thus, our discovered synthetic lethal interaction between NOTCH and JAK-STAT pathway may have crucial clinical significance. Combinatorial approach of targeting both NOTCH and JAK-STAT pathway has been tested for pancreatic cancer where these pathway are known to be activated in large number of patients and combined inhibition of the pathways was found to be superior to monotherapies in pancreatic cancer progression (68). Future investigations will be required to define the status of NOTCH and JAK-STAT-pathway in oral tumors to act as potential biomarker for adapting this promising combinatorial treatment strategy, targeting both these pathways as novel therapeutic approach. Moreover, the loss of function of NOTCH is also common in squamous cell carcinoma of skin, esophagus, uterine cervix, and lung. Thus, our findings may have wider implications in other cancers beyond the gingivobuccal oral cancer or HNSCC.

Conclusion

The genomic landscape of oral cancer suggest that this is mainly driven by tumor suppressor genes. Thus, developing mutation based targeted therapy is challenging. Therefore, alternative factors need be identified on which these cancer cells show dependencies in context to the loss of function of any of these specific tumor suppresser genes; as synthetic lethal approach. Since NOTCH-inactive gingivobuccal oral cancer cells showed dependency on JAK-STAT pathway for maintaining stemness, this may act as potential synthetic lethal target against stemness in gingivobuccal oral cancer with loss of function phenotype of NOTCH-pathway.

Materials And Methods

Cell lines and culture condition:

OSCC cell lines, GBC02 and its derivatives pLenti-GFP, hICN-GFP, hHes1-GFP and BHes1-GFP clones were cultured in Epilife with 2% FBS (GIBCO), 1X Antibiotic-Antimycotic (Anti-Anti),and supplemented with 1X B27 (Cat.#12587010; Thermo-Scientific), Hydrocortisone (0.4 µg/ml; Cat. #H6909; Merck), EGF (20 ng/ml; Cat.# PHG0311; Thermo-Scientific) and human basic FGF (20 ng/ml; Cat. # PHG0261; Thermo-Scientific). SCC029, SCC032 were cultured in Minimal Essential Medium (MEM) with 10% FBS and 1X Anti-Anti, SCC070 and derivatives pLenti-GFP, hICN-GFP, hHes1-GFP and BHes1-GFP clones were cultured in Dulbecco's Modified Eagle Medium (DMEM) with 10% FBS, and 1X Anti-Anti. The cells were cultured and maintained either in 60 mm/100mm plate or T-25 flasks as an adherent monolayer at 37°C in a 5% CO_2 atmosphere in respective culture media. All cell lines were maintained at their logarithmic phase of

growth before each experiment and plated when it reached 70% of confluency. Lower passage cell lines were used for the experiments.

3D-spheroid culture of OSCC cell lines:

GBC02, SCC029, SCC032, SCC070 and the respective derived clone cells were plated at a density of 5000 cells/mL in cell line specific 1X growth factor media as mentioned in the cell culture section and were supplemented with 1X B-27 (Cat.#12587010; Thermo-Scientific), Hydrocortisone (0.4 µg/ml; Cat. #H6909; Merck), EGF (20 ng/ml; Cat.# PHG0311; Thermo-Scientific) and human basic FGF (20 ng/ml; Cat. # PHG0261; Thermo-Scientific) in 1.25% Geltrex (Cat. # A14132-02, Invitrogen) for 3D-spheroid cultures in 96-well or 6-well ultra-low attachment plate (Corning). On every alternate day the spheres were supplemented with 5X growth factor media. As indicated, drugs were either added along with the seeding of the cells or on 5^{th} day of generation of 3D-sphere with average diameter of 60µm. Images have been taken every day during the experiment using inverted phase contrast microscope (CKX41SF, Olympus) and by EVOS-M7000 (Cat#AMF7000, Thermo fisher Scientific) fluorescence microscope. All Images are the representative of multiple fields taken at 10X magnification. Bar represents 275µm. Individual 3D-sphere diameter has been measured by ImageJ software (ImageJ 1.50e).

RNA extraction, cDNA preparation and qRT-PCR:

The 3D-sphere was collected by centrifugation at 800g for 5 minutes. 3D-sphere pellet was immediately lysed in RLT-plus buffer (RNA-Easy plus kit, Qiagen) with beta-mercaptoethanol. Total RNA was extracted using RNA-Easy plus kit (Cat#74034, Qiagen) as per the manufacturer's instructions. Extracted total-RNA was quantified using the Nanodrop quantification system (Thermo-Scientific). 500 ng of total RNA was converted to cDNA using Verso cDNA synthesis Kit (Cat# AB1453A, Thermo-Scientific) according to the instructions of the manufacturer. 1/20th of the cDNA has been used for Real-Time PCR which was performed on BioRad CFX96 Real-Time PCR system (BioRad) Using SsoEva Green SYBR mix (Cat# 172-5203, BioRad). The gene expression level was normalized with housekeeping gene GAPDH as endogenous reference and plotted as relative normalized expression with the help of CFX96 Maestro software (BioRad). Primers used for the real-time PCR analysis were as tabulated.

RNA sequencing and pathway analysis:

The bulk RNA sequencing was done using Illumina HiSeq2500. Quality assessment was done by using Agilent Bio-analyser 2100 with Agilent nano kit. Library was prepared using TruSeq Standard Total RNA Library prep kit. Generated data was processed by the core facility of National Institute of Biomedical Genomics (NIBMG), Kalyani. Significant (p value ≤ 0.05) differentially upregulated and downregulated (log2 fold change ≥ 2)) genes were analyzed for pathway enrichment by Gene Set Enrichment Analysis (GSEA) and Cytoscape software.

Small molecule inhibitors and siRNA:

LY4575 and RO4929097, the gamma-secretase inhibitors, and Ruxolitinib (INCB08424)- inhibitors for JAK1/2, and Tofacitinib (CP-690550) inhibitors for JAK3 were purchased from selleckchem. were also obtained from selleckchem. For in-vitro experiments LY, RO, Tofacitinib and Ruxolitinib were prepared as a 10mM stock in dimethyl sulfoxide (DMSO) (Sigma). For treatment of LY, RO, Tofacitinib, Ruxolitinib the 5μM and in combination 5μM+5μM concentrations were used, DMSO was used as vehicle control. For siRNA mediated transient knock-down, cells were seeded a day before and on the next day interferin mediated transfection was performed with respective siRNA. The siControl was kept as negative control for the protocol. The knock-down efficiency was assessed by qRT-PCR for each siRNA.

Lentivectors and Transduction of OSCC cell lines:

To mimic the genetically active and inactive state of Notch pathway in-vitro we have generated Constitutive Notch pathway active and in-active OSCC clones were generated by lentivector mediated transduction of PLenti.CMV.GFP.Puro (Addgene#17488), EF.hHES1.Ubc.GFP (Addgene#17624), EF.deltaBHES1.Ubc.GFP (Addgene#24982), EF.hICN1.Ubc.GFP (Addgene#17626). Recombinant Lentivectors were produced by transient transfection of transducing vectors into HEK293T cells with packaging vectors, a plasmid expressing the HIV-1 gag/pol, tat, and rev genes. Lentivector transfection and efficiency was validated by GFP reporter expression in fluorescence microscopy, FACS based phenotyping and mRNA expression was assessed by qRT-PCR. To get the pure population of the transduced cells, cells were GFP sorted and expanded.

MTT assay:

IC50 of cisplatin was measured by MTT assay. 4000 cells per well are seeded in triplicates in 96 well culture plates (Eppendorf) for each condition. On next day cisplatin was added along with the Notch pathway inhibitors and kept for another 72 hours (3 days). On day 4, 10 μl of MTT reagent (Cat # M5655; Sigma) is directly added into the wells at final concentration of 1 mg/ml and incubated for 4 hours. Later, media is removed completely from each well and the developed formazan crystal is dissolved in DMSO. The triplicate absorbance values are recorded using softmax pro software on Spectramax (SpectraMax M2) and IC50 values were calculated based on the viability of the control and treated cells.

CT-Violet dye dilution assay:

Cells were acquired at 70% of confluency and stained with CT-Violet dye (Cat # C34557, Invitrogen) as per the manufactures protocol. $1x10^5$ stained cells were processed for FACS based analysis of baseline fluorescence at Day 0 for CT-Violet staining in BV421 channel using flow cytometry. Rest of the cells were allowed to proliferate for 4 days and subsequently subjected to flow cytometry based sorting. Cells were sorted as CT-Violet- High or - Low cells from the stained population, by making gates for 10% top and bottom stained cells, respectively. These cells were plated for sphere formation as well as collected for qRT-PCR based analysis of mRNA expressions.

AlamarBlue assay:

To follow the viability of 3D-spheres after the treatment duration, 10ul of AlamarBlue dye (AlamarBlue, Cell Viability Assay, Cat# DAL1025, Life Technologies) was added in a 100 ml 3D-sphere containing culture medium in the 96 well ultra-low attachment plates. On next day (~14 hrs incubation) 80ul from each well was collected in Flat Bottom black polystyrene assay plate (Costar Cat # 3915, Corning) and the fluorescence reading was taken by using 560 nm wave length of excitation and 590 nm for emission wave length using Spectramax (SpectraMax M2).

Western blotting:

Cells and spheres from control and treated conditions were twice washed with chilled (4°C) PBS and were lysed in RIPA buffer (50 mM Tris-HCl pH 7.4, 150 mM NaCl, 1mM EDTA, 0.5 % sodium deoxycolate, 0.1% SDS, and 1% Triton X-100 with freshly added 1X sodium vanadate, 1X protease and phosphatase inhibitors). Lysates were incubated on ice for 30 min with vortex at every 5 minutes followed by centrifugation at 10,000*g* for 20 min at 4°C. Supernatants were collected in fresh prechilled tubes as total protein lysate sample. Protein concentrations were estimated with the BCA protein assay kit (Pierce, 23227). For each sample, 30 µg of lysates were boiled at 95°C in the DTT containing 1X gel loading, reducing buffer and samples were separated on a 10% Bis-acrylamide gel and transferred onto a nitrocellulose membrane. 5% non-fat dried milk in TBST was used to block the membrane for 1 hour at room temperature, and immunoblotted overnight at 4°C using primary antibodies diluted in TBST. Following the incubations with primary antibodies, membranes were incubated with either horseradish peroxidase (HRP)-conjugated secondary anti-mouse-IgG (Invitrogen-Cat#31430) or anti-rabbit-IgG (Invitrogen-Cat#31460) antibodies. Membranes were developed with ECL substrate for imaging by BioRad ChemiDoc.

Zebrafish xenograft:

Experiments with Zebrafish were approved as per the guidelines of Government of India. Zebrafish (AB/Tuebingen) embryo of 48 hours post fertilization (hpf) were maintained in the 1X E3 medium (5 mM NaCl 0.17 mM KCl 0.33 mM $CaCl_2$ 0.33 mM $MgSO_4$ 5 % methylene blue), were dechorionated manually and were treated in the anaesthetic Tricaine (3-amino benzoic acid ethyl ester). Anesthetized embryos were placed in a grooved petri dish containing solidified 1XE3-agarose. GFP positive OSCC cells from experimental conditions were injected at 100 cells/ 5nL into the yolk sac cavity of the embryos by Eppendorf's electronic microinjectors FemtoJet 4i (**FemtoJet® 4i**, Cat#5252000013). Post injection, embryos were maintained in a 32°C incubator, to facilitate the growth of human cells in embryos. Fishes were monitored and deaths were recorded for a maximum period seven days post injection. Fluorescent imaging was performed using EVOS M7000 and Nikon laser scanning confocal microscopy after anesthetizing using tricaine solution. For survivability analysis of the Zebrafish embryos, live or dead embryos were tabulated as 1 or 0 against day 0, 3, 5, 7 post injection of OSCC cells for each conditions. The survivability analysis and graphs were generated by ‘survival curve in survival analysis’ option in GraphPad prism software.

Quantification and statistical analysis:

All quantitative data were presented as means ± S.E.M from experiments performed in triplicates and from two or three biological repeats. Statistical analysis was performed using two-sided paired or unpaired t-tests. p values ≤ 0.05 were considered statistically significant. All the statistical details of experiments can be found in the respective methodology and figure legends.

List of primary antibody used in the study:

Antibody	Source	Identifier
Beta-Actin Mouse monoclonal	Abcam	ab8226
NOTCH1-activated Rabbit polyclonal	Abcam	ab8925
HES1 Rabbit polyclonal	Abcam	ab71559
SOX2 Rabbit polyclonal	Abcam	ab97959
SOX9 Rabbit polyclonal	Abcam	Ab26414
Jak1 Rabbit monoclonal	Cell Signaling	3344
Phospho-Jak1 Rabbit monoclonal	Cell Signaling	74129
Jak2 Rabbimonoclonal	Cell Signaling	3230
Phospho-Jak2 Rabbit monoclonal	Cell Signaling	8082
Jak3 Rabbit monoclonal	Cell Signaling	8827
Phospho-Jak3 Rabbit monoclonal	Cell Signaling	5031
STAT1 Rabbit polyclonal	Abclonal	A12075
Phospho-STAT1 Rabbit polyclonal	Abclonal	AP0453
STAT3 Rabbit polyclonal	Abclonal	A1192
Phospho-STAT3 Rabbit polyclonal	Abclonal	AP0070
STAT4 Rabbit polyclonal	Abclonal	A6991
Phospho-STAT4 Rabbit polyclonal	Abclonal	AP0137

List of primers (F= forward and R= reverse primer) used in the study

Sl. No.	Gene	Primer sequence (5’-3’)
1	18s_F	GTAACCCGTTGAACCCATT
	18s_R	CCATCCAATCGGTAGTAGCG
2	GAPDH_F	GGTGGTCTCCTCTGACTTCAACA
	GAPDH_R	GTTGCTGTAGCCAAATTCGTTGT
3	ABCG2_F	CACAAGGAAACACCAATGGCT
	ABCG2_R	ACAGCTCCTTCAGTAAATGCCTTC
4	ALDH1A1_F	GATGCCGACTTGGACAATGC
	ALDH1A1_R	TCTTAGCCCGCTCAACACTC
5	Nanog_F	CAGCCCCGATTCTTCCACCAGTCCC
	Nanog_R	CGGAAGATTCCCAGTCGGGTTCACC
6	MYC _F	GGACCCGCTTCTCTGAAAGG
	MYC_R	TAACGTTGAGGGGCATCGTC
7	KLF4_F	GGACACAGGGGATGATGC
	KLF4_R	CGCGTAATCACAAGTGTG
8	Oct4_F	GACAGGGGGAGGGGAGGAGCTAGG
	Oct4_R	CTTCCCTCCAACCAGTTGCCCCAAAC
9	SOX2_F	AGTATCAGGAGTTGTCAAGGC
	SOX2_R	AGTCCTAGTCTTAAAGAGGCA
10	SOX9_F	CCTGCCCGTTCTTCACCGAC
	SOX9_R	GCTCTGGAGACTTCTGAACGAGAGC
11	CK1_F	GATTGCCACCTACAGGACCC
	CK1_R	ACAGACACACTCACGTTCGG
12	CK5_F	ATCACCGTTCCTGGGTAACA
	CK5_R	AGGCACTAGTGGGTTGGGAG
13	CK10_F	AGAAGGTCGCTACTGTGTGC
	CK10_R	TTCTGGCACTCGGTTTCAGC
14	CK14_F	CCCAGTTCTCCTCTGGATCG
	CK14_R	GCAGGAGAGGGGATCTTCCA

Declarations

Author contributions:

SG conceptualized the project, developed methodology, performed experiments and analysed data, drafted the manuscript. PM performed bioinformatic investigation and analysed data, performed statistical analysis, corrected manuscript draft. US participated in investigations and analysis, corrected manuscript draft. AG performed RNAseq data analysis. NKB performed RNAseq data analysis, performed statistical analysis, corrected manuscript draft. SSR performed zebrafish xenograft experiments. MA participated in formal analysis of zebrafish xenograft experiments. SS Conceptualized the work, obtained funding, drafted and corrected the manuscript. All authors reviewed and approved the final manuscript.

Acknowledgement:

This work is supported by the grant (CRG/2021/005556) received from DST-SERB and intramural funds from NIBMG to SS. SG acknowledges DBT, PM Acknowledges CSIR and US acknowledges DBT-NIBMG for fellowship support. We thank Professors Saumitra Das and Dr. Kartiki Desai for scientific discussions and Dr. Arindam Maitra for assistance with transcriptomics platform.

Ethics approval and consent to participate:

Necessary permissions were obtained for performing all experiments.

Consent for publication:

All authors agree for publication of this manuscript

Availability of data and material:

All reported data and materials are available from the corresponding author, upon request.

Competing interests:

The authors declare no potential competing interest

Funding:

This work is supported by the grant (CRG/2021/005556) received from DST-SERB and intramural funds from NIBMG to SS

References

1. Sharma S, Satyanarayana L, Asthana S, Shivalingesh KK, Goutham BS, Ramachandra S. Oral cancer statistics in India on the basis of first report of 29 population-based cancer registries. J Oral Maxillofac Pathol. 2018;22(1):18–26.

2. Varshitha A. Prevalence of oral cancer in India. J Pharm Sci Res. 2015;7(10):845–8.
3. Coelho KR. Challenges of the oral cancer burden in India. J Cancer Epidemiol. 2012;
4. Mummudi N, Agarwal JP, Chatterjee S, Mallick I, Ghosh-Laskar S. Oral Cavity Cancer in the Indian Subcontinent – Challenges and Opportunities. Clin Oncol. 2019;31(8):520–8.
5. Misra S, Chaturvedi A, England NMS of, 2008 undefined. Management of gingivobuccal complex cancer. publishing.rcseng.ac.uk. 2008 Oct;90(7):546–53.
6. Tandon P, Dadhich A, Saluja H, Bawane S, Sachdeva S. The prevalence of squamous cell carcinoma in different sites of oral cavity at our Rural Health Care Centre in Loni, Maharashtra–a retrospective 10-year study. termedia.pl. 2017;21(2):178–83.
7. Durr ML, Van Zante A, Li D, Kezirian EJ, Wang SJ. Oral tongue squamous cell carcinoma in never-smokers: Analysis of clinicopathologic characteristics and survival. Otolaryngol - Head Neck Surg (United States). 2013 Jul;149(1):89–96.
8. Llewellyn CD, Johnson NW, Warnakulasuriya KAAS. Risk factors for squamous cell carcinoma of the oral cavity in young people - A comprehensive literature review. Oral Oncol. 2001;37(5):401–18.
9. Nguyen L V., Vanner R, Dirks P, Eaves CJ. Cancer stem cells: An evolving concept. Nat Rev Cancer. 2012;12(2):133–43.
10. Pattabiraman DR, Weinberg RA. Tackling the cancer stem cells-what challenges do they pose? Nat Rev Drug Discov. 2014;13(7):497–512.
11. Plaks V, Kong N, Werb Z. The cancer stem cell niche: How essential is the niche in regulating stemness of tumor cells? Cell Stem Cell. 2015;16(3):225–38.
12. Kaiser J. The cancer stem cell gamble. Science (80-). 2015 Jan 16;347(6219):226–9.
13. Gasch C, Ffrench B, O'Leary JJ, Gallagher MF. Catching moving targets: Cancer stem cell hierarchies, therapy-resistance & considerations for clinical intervention. Mol Cancer. 2017 Feb 23;16(1).
14. Bertolini G, Roz L, Perego P, Tortoreto M, Fontanella E, Gatti L, et al. Highly tumorigenic lung cancer CD133+ cells display stem-like features and are spared by cisplatin treatment. Proc Natl Acad Sci U S A. 2009 Sep 22;106(38):16281–6.
15. Agrawal N, Frederick MJ, Pickering CR, Bettegowda C, Chang K, Li RJ, et al. Exome sequencing of head and neck squamous cell carcinoma reveals inactivating mutations in NOTCH1. Science (80-). 2011 Aug 26;333(6046):1154–7.
16. Stransky N, Egloff AM, Tward AD, Kostic AD, Cibulskis K, Sivachenko A, et al. The mutational landscape of head and neck squamous cell carcinoma. Science (80-). 2011 Aug 26;333(6046):1157–60.
17. Pickering CR, Zhang J, Yoo SY, Bengtsson L, Moorthy S, Neskey DM, et al. Integrative genomic characterization of oral squamous cell carcinoma identifies frequent somatic drivers. Cancer Discov. 2013;3(7):770–81.
18. Committee W. Pan-cancer analysis of whole genomes Pan-cancer analysis of whole genomes. bioRxiv. 1969;3(June):162784.

19. Maitra A, Biswas NK, Amin K, Kowtal P, Kumar S, Das S, et al. Mutational landscape of gingivo-buccal oral squamous cell carcinoma reveals new recurrently-mutated genes and molecular subgroups. Nat Commun. 2013;4.
20. Shah PA, Huang C, Li Q, Kazi SA, Byers LA, Wang J, et al. NOTCH1 Signaling in Head and Neck Squamous Cell Carcinoma. Cells. 2020;9(12).
21. Fukusumi T, Califano JA. The NOTCH Pathway in Head and Neck Squamous Cell Carcinoma. J Dent Res. 2018;97(6):645–53.
22. Nicolas M, Wolfer A, Raj K, Kummer JA, Mill P, Van Noort M, et al. Notch1 functions as a tumor suppressor in mouse skin. Nat Genet. 2003;33(3):416–21.
23. Proweller A, Tu L, Lepore JJ, Cheng L, Lu MM, Seykora J, et al. Impaired notch signaling promotes De novo squamous cell carcinoma formation. Cancer Res. 2006;66(15):7438–44.
24. Leethanakul C, Patel V, Gillespie J, Pallente M, Ensley JF, Koontongkaew S, et al. Distinct pattern of expression of differentiation and growth-related genes in squamous cell carcinomas of the head and neck revealed by the use of laser capture microdissection and cDNA arrays. Oncogene. 2000;19(28):3220–4.
25. Zhang T-H, Liu H-C, Zhu L-J, Chu M, Liang Y-J, Liang L-Z, et al. Activation of Notch signaling in human tongue carcinoma. Wiley Online Libr. 2011 Jan;40(1):37–45.
26. Yoshida R, Nagata M, Nakayama H, Niimori-Kita K, Hassan W, Tanaka T, et al. The pathological significance of Notch1 in oral squamous cell carcinoma. Lab Investig. 2013;93(10):1068–81.
27. Hijioka H, Setoguchi T, Miyawaki A, Gao H, Ishida T, Komiya S, et al. Upregulation of Notch pathway molecules in oral squamous cell carcinoma. Int J Oncol. 2010;36(4):817–22.
28. Wirth M, Doescher J, Jira D, Meier MA, Piontek G, Reiter R, et al. HES1 mRNA expression is associated with survival in sinonasal squamous cell carcinoma. Oral Surg Oral Med Oral Pathol Oral Radiol. 2016;122(4):491–9.
29. Sun W, Gaykalova DA, Ochs MF, Mambo E, Arnaoutakis D, Liu Y, et al. Activation of the NOTCH pathway in head and neck cancer. Cancer Res. 2014;74(4):1091–104.
30. Upadhyay P, Nair S, Kaur E, Aich J, Dani P, Sethunath V, et al. Notch pathway activation is essential for maintenance of stem-like cells in early tongue cancer. Oncotarget. 2016;7(31):50437–49.
31. Lee SH, Hong HS, Liu ZX, Kim RH, Kang MK, Park NH, et al. TNFα enhances cancer stem cell-like phenotype via Notch-Hes1 activation in oral squamous cell carcinoma cells. Biochem Biophys Res Commun. 2012;424(1):58–64.
32. Rettig EM, Bishop JA, Agrawal N, Chung CH, Sharma R, Zamuner F, et al. HEY1 is expressed independent of NOTCH1 and is associated with poor prognosis in head and neck squamous cell carcinoma. Oral Oncol. 2018;82:168–75.
33. Facompre N, Nakagawa H, Herlyn M, Basu D. Stem-Like Cells and Therapy Resistance in Squamous Cell Carcinomas. Adv Pharmacol. 2012;65:235–65.

34. Peitzsch C, Nathansen J, Schniewind SI, Schwarz F, Dubrovska A. Cancer stem cells in head and neck squamous cell carcinoma: Identification, characterization and clinical implications. Cancers (Basel). 2019;11(5).
35. Yang L, Shi P, Zhao G, Xu J, Peng W, Zhang J, et al. Targeting cancer stem cell pathways for cancer therapy. Signal Transduct Target Ther. 2020;5(1).
36. Baillie R, Tan ST, Itinteang T. Cancer stem cells in oral cavity squamous cell carcinoma: A review. Front Oncol. 2017 Jun 2;7(JUN).
37. Li W, Ma H, Zhang J, Zhu L, Wang C, Yang Y. Unraveling the roles of CD44/CD24 and ALDH1 as cancer stem cell markers in tumorigenesis and metastasis. Sci Rep. 2017;7(1).
38. Vipparthi K, Hari K, Chakraborty P, Ghosh S, Patel AK, Ghosh A, et al. Emergence of hybrid states of stem-like cancer cells correlates with poor prognosis in oral cancer. iScience. 2022;25(5):104317.
39. Zhang Z-P, Sun Y-L, Fu L, Gu F, Zhang L, Hao X-S. Correlation of Notch1 expression and activation to cisplatin-sensitivity of head and neck squamous cell carcinoma. Ai Zheng. 2009;28(2):100–3.
40. Gu F, Ma Y, Zhang Z, Zhao J, Kobayashi H, Zhang L, et al. Expression of Stat3 and Notch1 is associated with cisplatin resistance in head and neck squamous cell carcinoma. Oncol Rep. 2010;23(3):671–6.
41. Cole AJ, Fayomi AP, Anyaeche VI, Bai S, Buckanovich RJ. An evolving paradigm of cancer stem cell hierarchies: therapeutic implications. Theranostics. 2020;10(7):3083–98.
42. Bonnet D, Dick JE. Human acute myeloid leukemia is organized as a hierarchy that originates from a primitive hematopoietic cell. Nat Med. 1997 Jul;3(7):730–7.
43. Gupta PB, Fillmore CM, Jiang G, Shapira SD, Tao K, Kuperwasser C, et al. Stochastic state transitions give rise to phenotypic equilibrium in populations of cancer cells. Cell. 2011 Aug;146(4):633–44.
44. Dirkse A, Golebiewska A, Buder T, Nazarov P V, Muller A, Poovathingal S, et al. Stem cell-associated heterogeneity in Glioblastoma results from intrinsic tumor plasticity shaped by the microenvironment. Nat Commun. 2019 Apr;10(1):1787.
45. F Quail D, J Taylor M, Postovit L-M. Microenvironmental regulation of cancer stem cell phenotypes. Curr Stem Cell Res Ther. 2012;7(3):197–216.
46. Chaffer CL, Weinberg RA. How does multistep tumorigenesis really proceed? Cancer Discov. 2015;5(1):22–4.
47. Jones KB, Furukawa S, Marangoni P, Ma H, Pinkard H, D'Urso R, et al. Quantitative clonal analysis and single-cell transcriptomics reveal division kinetics, hierarchy, and fate of oral epithelial progenitor cells. Cell Stem Cell. 2019;24(1):183–92.
48. Lim KJ, Brandt WD, Heth JA, Muraszko KM, Fan X, Bar EE, et al. Lateral inhibition of Notch signaling in neoplastic cells. Oncotarget. 2015;6(3):1666.
49. Ryan N, Anderson K, Volpedo G, Hamza O, Varikuti S, Satoskar AR, et al. STAT1 inhibits T-cell exhaustion and myeloid derived suppressor cell accumulation to promote antitumor immune responses in head and neck squamous cell carcinoma. Int J cancer. 2020;146(6):1717–29.

50. Pectasides E, Egloff A-M, Sasaki C, Kountourakis P, Burtness B, Fountzilas G, et al. Nuclear Localization of Signal Transducer and Activator of Transcription 3 in Head and Neck Squamous Cell Carcinoma Is Associated with a Better PrognosisSTAT3 and Prognosis in HNSCC. Clin Cancer Res. 2010;16(8):2427–34.
51. Rao SK, Pavicevic Z, Du Z, Kim J-G, Fan M, Jiao Y, et al. Pro-inflammatory genes as biomarkers and therapeutic targets in oral squamous cell carcinoma. J Biol Chem. 2010;285(42):32512–21.
52. Concha-Benavente F, Srivastava RM, Trivedi S, Lei Y, Chandran U, Seethala RR, et al. Identification of the Cell-Intrinsic and-Extrinsic Pathways Downstream of EGFR and IFNγ That Induce PD-L1 Expression in Head and Neck CancerEGFR/IFNγ-Mediated PD-L1 Expression Is JAK2–STAT1 Dependent. Cancer Res. 2016;76(5):1031–43.
53. Thomas SJ, Snowden JA, Zeidler MP, Danson SJ. The role of JAK/STAT signalling in the pathogenesis, prognosis and treatment of solid tumours. Br J Cancer. 2015;113(3):365–71.
54. Shih CH, Chang YJ, Huang WC, Jang TH, Kung H-J, Wang WC, et al. EZH2-mediated upregulation of ROS1 oncogene promotes oral cancer metastasis. Oncogene. 2017;36(47):6542–54.
55. Shibue T, Weinberg RA. EMT, CSCs, and drug resistance: the mechanistic link and clinical implications. Nat Rev Clin Oncol. 2017;14(10):611–29.
56. Dongre A, Rashidian M, Reinhardt F, Bagnato A, Keckesova Z, Ploegh HL, et al. Epithelial-to-mesenchymal transition contributes to immunosuppression in breast carcinomas. Cancer Res. 2017;77(15):3982–9.
57. Doherty MR, Parvani JG, Tamagno I, Junk DJ, Bryson BL, Cheon HJ, et al. The opposing effects of interferon-beta and oncostatin-M as regulators of cancer stem cell plasticity in triple-negative breast cancer. Breast Cancer Res. 2019;21(1):1–12.
58. Jin W. Role of JAK/STAT3 signaling in the regulation of metastasis, the transition of cancer stem cells, and chemoresistance of cancer by epithelial–mesenchymal transition. Cells. 2020;9(1):217.
59. Ko J, Kim J-Y, Kim BR, Lee EJ, Kikkawa DO, Yoon JS. Signal transducer and activator of transcription 3 as a potential therapeutic target for Graves' orbitopathy. Mol Cell Endocrinol. 2021;534:111363.
60. Yang Z, Guo L, Liu D, Sun L, Chen H, Deng Q, et al. Acquisition of resistance to trastuzumab in gastric cancer cells is associated with activation of IL-6/STAT3/Jagged-1/Notch positive feedback loop. Oncotarget. 2015;6(7):5072.
61. Ngo KT, Wang J, Junker M, Kriz S, Vo G, Asem B, et al. Concomitant requirement for Notch and Jak/Stat signaling during neuro-epithelial differentiation in the Drosophila optic lobe. Dev Biol. 2010;346(2):284–95.
62. Beebe K, Lee W-C, Micchelli CA. JAK/STAT signaling coordinates stem cell proliferation and multilineage differentiation in the Drosophila intestinal stem cell lineage. Dev Biol. 2010;338(1):28–37.
63. Jiang H, Patel PH, Kohlmaier A, Grenley MO, McEwen DG, Edgar BA. Cytokine/Jak/Stat signaling mediates regeneration and homeostasis in the Drosophila midgut. Cell. 2009;137(7):1343–55.

64. Assa-Kunik E, Torres IL, Schejter ED, St Johnston D, Shilo BZ. Drosophila follicle cells are patterned by multiple levels of Notch signaling and antagonism between the Notch and JAK/STAT pathways. Development. 2007;134(6):1161–9.
65. Kamakura S, Oishi K, Yoshimatsu T, Nakafuku M, Masuyama N, Gotoh Y. Notch1 activation in the molecular pathogenesis of T-cell acute lymphoblastic leukemia. Nat Cell Biol. 2004;6:547–54.
66. Jin S, Mutvei AP, Chivukula I V, Andersson ER, Ramsköld D, Sandberg R, et al. Non-canonical Notch signaling activates IL-6/JAK/STAT signaling in breast tumor cells and is controlled by p53 and IKKα/IKKβ. Oncogene. 2013;32(41):4892–902.
67. Loganathan SK, Schleicher K, Malik A, Quevedo R, Langille E, Teng K, et al. Rare driver mutations in head and neck squamous cell carcinomas converge on NOTCH signaling. Science (80-). 2020;367(6483):1264–9.
68. Palagani V, Bozko P. El khatib M, Belahmer H, Giese N, Sipos B, et al. Comb Inhib Notch JAK/STAT is Super to monotherapies Impair Pancreat cancer Progress Carcinog. 2014;35(4):859–66.

Figures

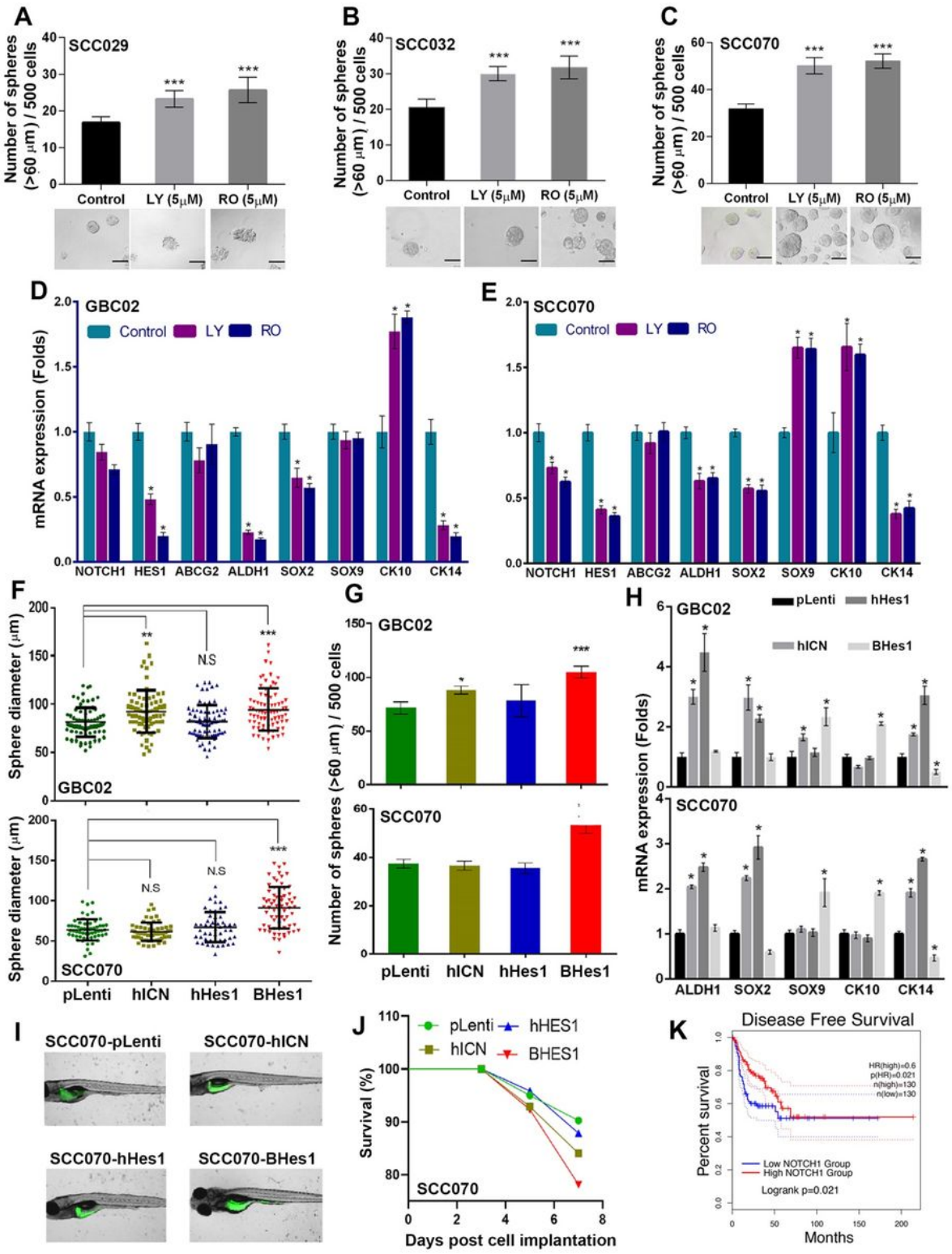

Figure 1

Maintenance of stemness in both NOTCH-pathway active and inactive Oral-SLCCs.

A-C. Average sphere number (>60 μm) in LY and RO treatment compared to DMSO (0.01%) control in SCC029, SCC032 and SCC070 cell lines and the lower panel of the bar graphs shows the representative bright field images from each treatment condition of the respective cell lines, scale bar= 60μm. **D,E.**

Relative normalized mRNA expression of *NOTCH1, HES1, ABCG2, ALDH1, SOX2, SOX9, CK10* and *CK14* in Control (0.01% DMSO) and LY, RO treated spheres of GBC02 and SCC070by qRT-PCR. **F.** The dot plots represents the sphere diameter (µm) distribution in pLenti, hICN, hHes1 and BHes1 clone cells of GBC02 and SCC070 cell lines **G.**The bar graphs represent changes in average spheres numbers in pLenti, hICN, hHes1 and BHes1 clone cells of GBC02 and SCC070 cell lines. **H.** Relative normalized mRNA expression of *ALDH1, SOX2, SOX9, CK10* and *CK14* in pLenti, hHes1, hICN and BHes1 spheres of GBC02 and SCC070 by qRT-PCR **I.**Representative in-vivo zebrafish images, GFP regions shows the tumor formed from the injected GFP positive OSCC cells. **J.** The line graph shows the survivability of the zebrafish embryos injected with pLenti, hICN, hHes1 and BHes1 clone cells of SCC070. **K.** Survival analysis for NOTCH1-high or -low expressing HNSCC patients in TCGA-cohort, using GEPIA tool**.** * indicates *p*value < 0.05; ** indicates *p* value < 0.01; *** indicates *p*value < 0.001; N.S= Non-significant.

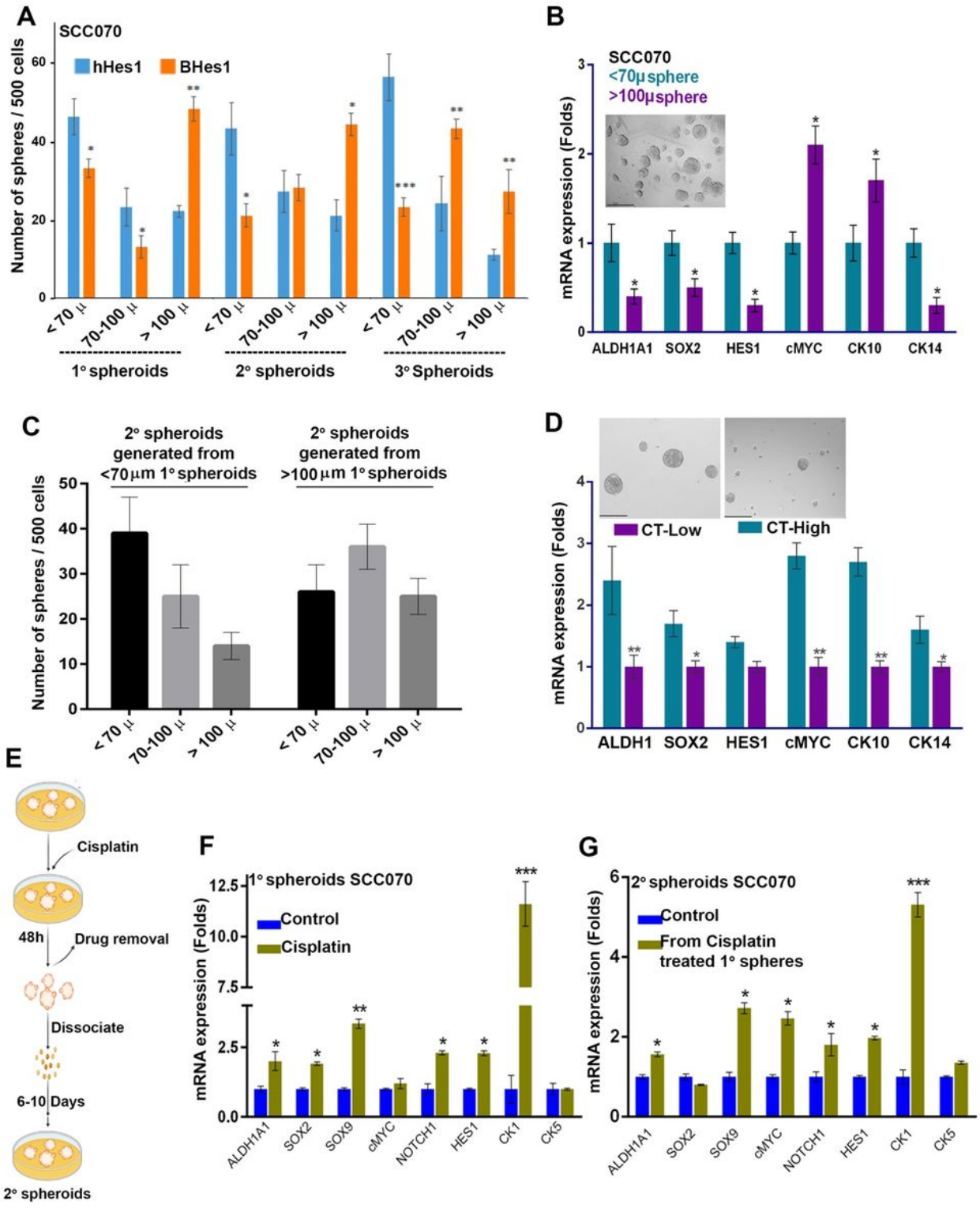

Figure 2

Plasticity between NOTCH-pathway active and inactive status of Oral-SLCCs. A. The bar graphs represents the categorized <70 µm, 70-100 µm and >100 µm of spheres into 1', 2' and 3' (primary, secondary and tertiary) spheres from hHes1 and BHes1 clones of SCC070 cells. **B.** Relative normalized mRNA expression changes of ALDH1A1, SOX2, HES1, cMYC, CK10 and CK14 in <70µm and >100µm spheres from SCC070 by qRT-PCR, scale bar= 60µm **C.** The bar graphs represents average sphere

numbers in 2’ (secondary) sphere culture from 1’ <70µm and >100µm spheres of SCC070 cells, scale bar= 60µm **D.** The relative normalized mRNA expression of ALDH1, SOX2, HES1, cMYC, CK10 and CK14 in CT violet low and high spheres generated from SCC070 cells. **E.** Schematic diagram of cisplatin treatment of 1’ spheres and, subsequent dissociation of primary spheres into single cells for 2’ sphere plating. **F-G.** Relative normalized mRNA expression changes of ALDH1A1, SOX2, SOX9, cMYC, NOTCH1, HES1, cMYC, CK1 and CK5 in control and cisplatin 1’ spheres and in 2’ spheres generated from 1’ control and cisplatin treated spheres of SCC070 by qRT-PCR. * indicates *p*value < 0.05; ** indicates *p* value < 0.01; *** indicates *p*value < 0.001; N.S= Non-significant.

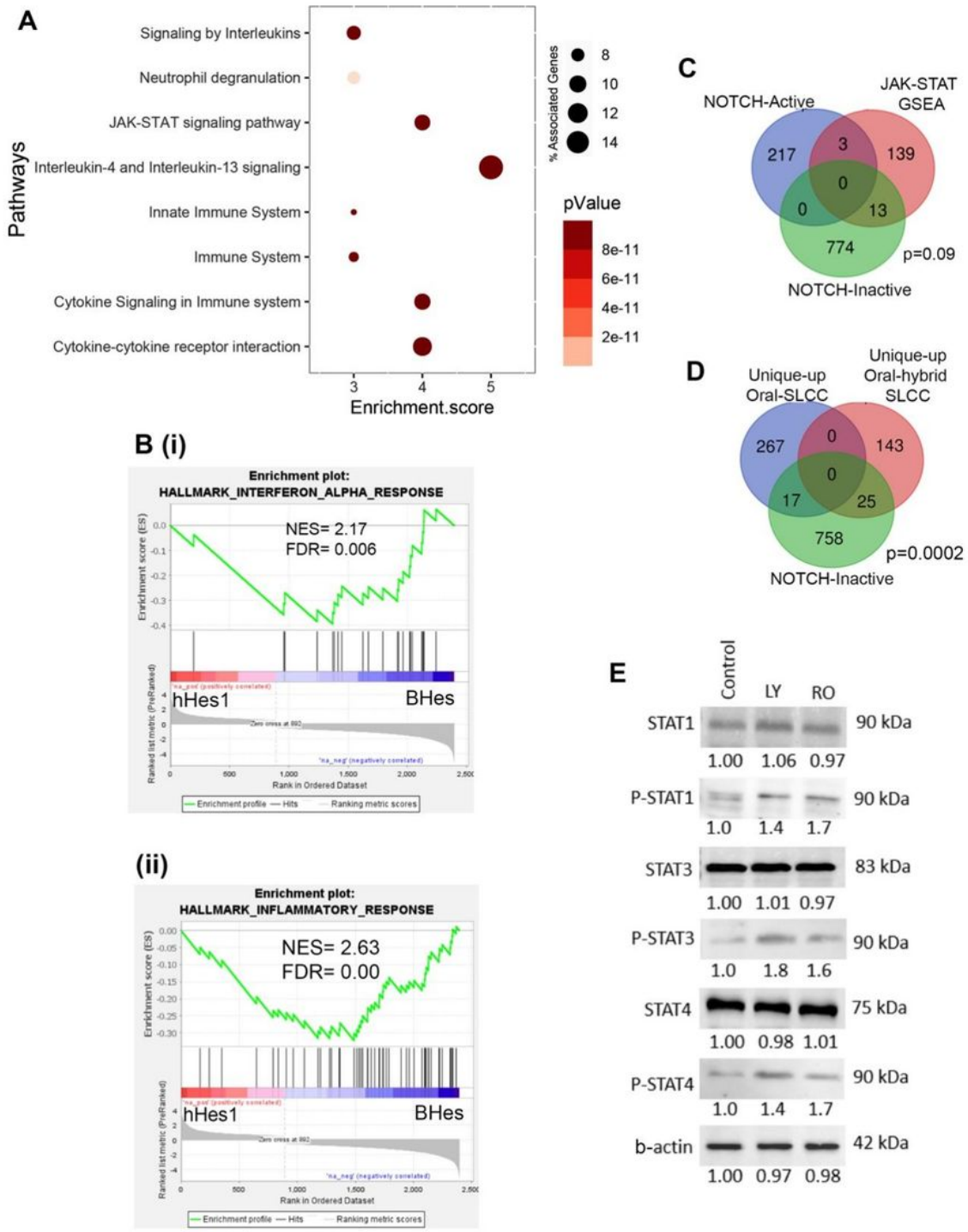

Figure 3

JAK-STAT pathway activation in NOTCH-inactive Oral-SLCCs: A. The pathway enrichment analysis has shown significant upregulation of top 8 biological pathways in Notch-inactiveBHes1 spheres. **B.i.** Gene Set Enrichment Analysis (GSEA) of differentially expressed genes between hHes1 and BHes1 spheres has shown significant enrichment of interferon response related genes **ii.** And of inflammatory response genes, in Notch-inactive BHes1 cells **C.** Venn diagram overlap of Notch-active, Notch-inactive and JAK-

STAT genes has shown significant co-expression of JAK-STAT genes in Notch-inactive Oral-SLCC l **D.**Comparison of gene expressions of unique-upregulated Oral-hybrid SLCC, which is more like progenitor in nature shown significant co-expression in Notch-inactive state compared to unique-upregulated genes in Oral-SLCC, which more like stem cells **E.**Western blots of JAK-STAT proteins in their original and phosphorylated state has shown upregulation of signaling activity in Notch inhibited spheres compared to the control.

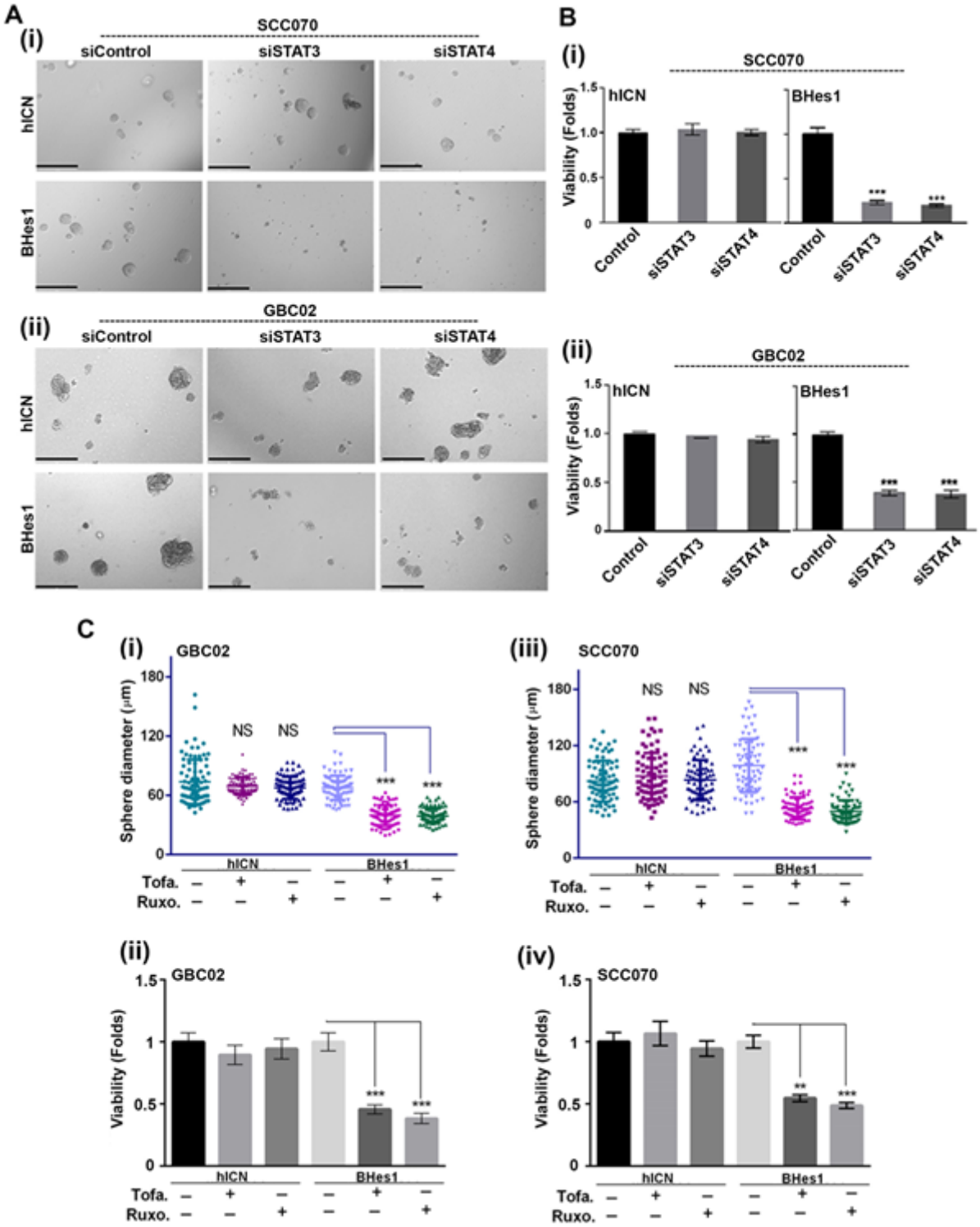

Figure 4

NOTCH-inactivated Oral-SLCCs shows dependency on JAK-STAT pathway. A. i-ii. Representative 10X images of the spheres from hICN and BHes1 cells of SCC070 and GBC02, treated with siSTAT3, siSTAT4. siControl was kept as control. scale bar= 275µm **B.i-ii.** The bar graphs shows changes in viability of hICN and BHes1 cells of SCC070 and GBC02, treated with siSTAT3, siSTAT4 and siControl was kept as control **C.i-iv.** The dot plots represents the sphere diameter distribution and viability changes in Tofa. and Ruxo. treated spheres of hICN and BHes1 cells from GBC02 (i-ii) and SCC070 (iii-iv) cell lines. * indicates *p* value < 0.05; ** indicates *p* value < 0.01; *** indicates *p* value < 0.001; N.S= Non-significant.

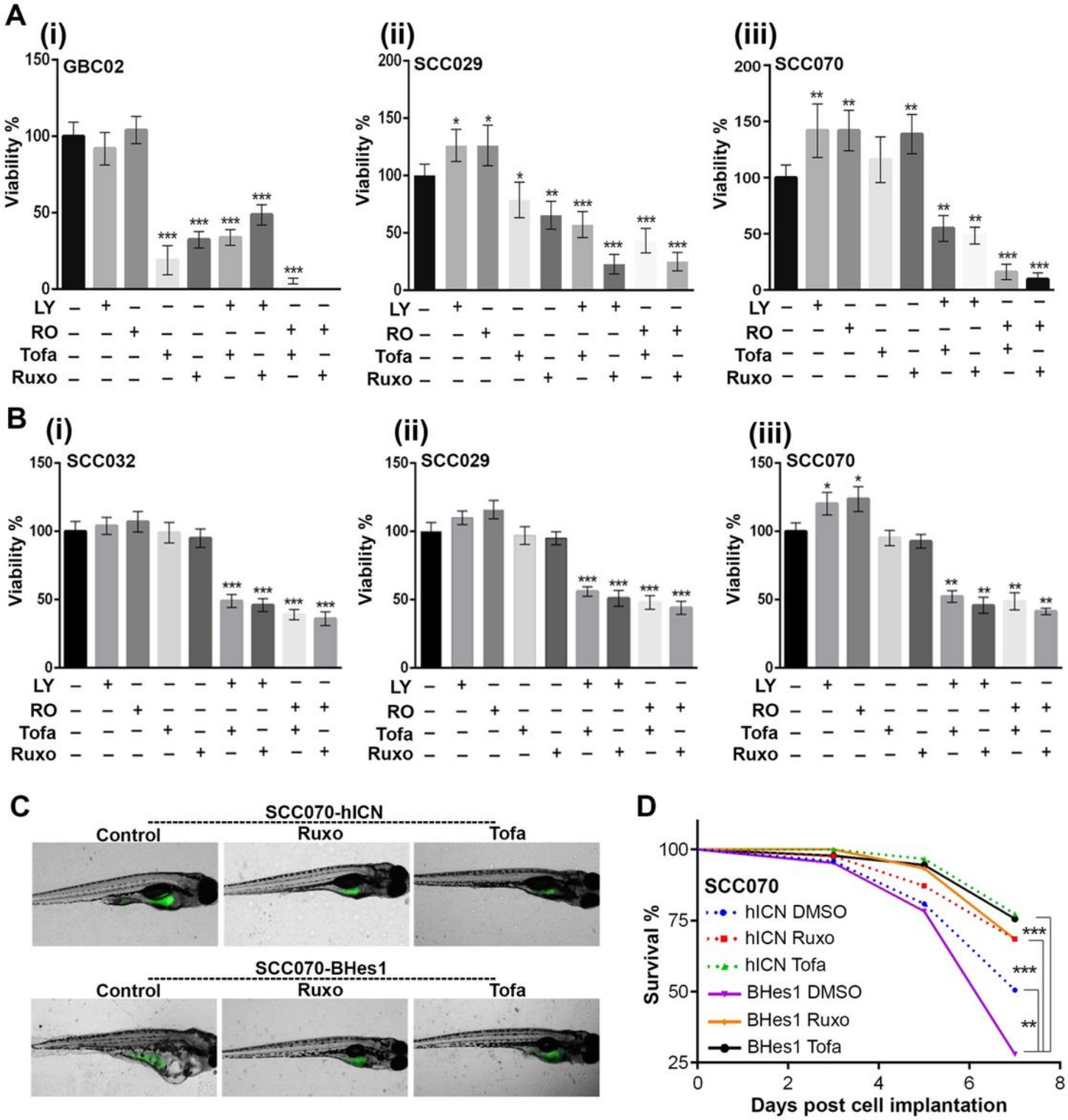

Figure 5

NOTCH-HES and JAK-STAT pathways acts in synthetic lethal manner: A. i-iii. The bar graphs represents viability of spheres of GBC02, SCC029 and SCC070 cell lines, where NOTCH-pathway was inhibited by LY and RO from the time of plating and JAK inhibitors, Tofa. and Ruxo. were added on 5th day of sphere formation and followed for another 48 hours. **B.i-iii.** The bar graphs represents viability of spheres of GBC02, SCC029 and SCC070 cell lines, where spheres were first allowed to generate and grow. On 5thday

of sphere formation Notch-pathway inhibitors (LY, RO) and JAK inhibitors (Tofa., Ruxo.) were added alone or in combination for 48 hrs. **C.** Representative in-vivo zebrafish images, where the GFP regions shows the tumor formed from the injected, Ruxo and Tofa pre-treated hICN or BHes1 clones of SCC070. **D.** The graph shows the survivability of the zebrafish embryos injected with Ruxo. and Tofa. pre-treated hICN and BHes1 cells of SCC070. *indicates *p* value < 0.05; ** indicates *p* value < 0.01; *** indicates *p* value < 0.001; N.S= Non-significant.

Supplementary Files

This is a list of supplementary files associated with this preprint. Click to download.

- SupplementaryData.pdf